ANTIOXIDANTS & REDOX SIGNALING
Volume 14, Number 4, 2011

DOI: 10.1089/ars.2010.3213

ORIGINAL RESEARCH COMMUNICATION

NADPH Oxidase 2 Mediates Intermittent Hypoxia-Induced Mitochondrial Complex I Inhibition: Relevance to Blood Pressure Changes in Rats

Shakil A. Khan,[1] Jayasri Nanduri,[1] Guoxiang Yuan,[1] Brian Kinsman,[1] Ganesh K. Kumar,[1] Joy Joseph,[2] Balaraman Kalyanaraman,[2] and Nanduri R. Prabhakar[1]

Abstract

Previous studies identified NADPH oxidases (Nox) and mitochondrial electron transport chain at complex I as major cellular sources of reactive oxygen species (ROS) mediating systemic and cellular responses to intermittent hypoxia (IH). In the present study, we investigated potential interactions between Nox and the mitochondrial complex I and assessed the contribution of mitochondrial ROS in IH-evoked elevation in blood pressure. IH treatment led to stimulus-dependent activation of Nox and inhibition of complex I activity in rat pheochromocytoma (PC)12 cells. After re-oxygenation, Nox activity returned to baseline values within 3 h, whereas the complex I activity remained downregulated even after 24 h. IH-induced complex I inhibition was prevented by Nox inhibitors, Nox2 but not Nox 4 siRNA, in cell cultures and was absent in $gp91^{phox-/Y}$ (Nox2 knock-out; KO) mice. Using pharmacological inhibitors, we show that ROS generated by Nox activation mobilizes Ca^{2+} flux from the cytosol to mitochondria, leading to S-glutathionylation of 75- and 50-kDa proteins of the complex I and inhibition of complex I activity, which results in elevated mitochondrial ROS. Systemic administration of mito-tempol prevented the sustained but not the acute elevations of blood pressure in IH-treated rats, suggesting that mitochondrial-derived ROS contribute to sustained elevation of blood pressure. *Antioxid. Redox Signal.* 14, 533–542.

Introduction

SLEEP DISORDERED BREATHING manifested as recurrent apneas is characterized by transient, repetitive cessations of breathing (~10–15 s in adults), resulting in periodic decreases in arterial blood O_2 or intermittent hypoxia (IH). Patients with recurrent apneas develop several comorbidities, including hypertension, sympathetic activation, and abnormalities of breathing. (24). Studies on adult and neonatal rodent models suggest that reactive oxygen species (ROS) mediate many of the systemic responses to IH, including hypertension, sympathetic activation [reviewed in refs. (29, 35)], alterations in carotid body function (26, 27, 30), increase in catecholamine secretion from the adrenal chromaffin cells (14, 33), and changes in breathing (25). In addition, ROS signaling has also been implicated in activation of transcriptional factors and second messengers in IH-treated cell cultures (38, 39). Together, these studies suggest that ROS signaling mediates systemic and cellular responses to IH.

Membrane or cytosolic oxidases are the major sources for enzymatic generation of ROS (18). Recent studies implicated NADPH oxidases (Nox), especially Nox2 (also called $gp91^{phox}$), in IH-evoked changes in sleep behavior (40), sensory long-term facilitation of the carotid body (27), and plasticity of respiratory behavior (22). Besides oxidases, mitochondrial electron transport chain complexes also generate ROS (17, 23). For instance, mitochondrial complex I (E.C 1.6.5.3, proton-translocating NADH:ubiquinone oxidoreductase), which is responsible for the oxidation of NADH by ubiquinone, is a major source of mitochondrial ROS (41). We have previously reported selective inhibition of mitochondrial complex I, but not the complex III in IH-treated rodents (27) and cell cultures (38). However, the mechanism(s) by which IH inhibits complex I activity have not been examined. Given that mitochondrial complex I activity can be altered by the redox state (32), we hypothesized that Nox activation and the resulting ROS mediates IH-induced inhibition of complex I. We tested this possibility in IH-treated cell cultures and mice deficient in Nox function. Our results demonstrate that ROS generated by Nox, especially Nox2, inhibit complex I activity *via* Ca^{2+}-dependent S-glutathionylation of complex I subunits resulting in elevated mitochondrial ROS levels. More

[1]Department of Medicine, Center for Systems Biology of O_2 Sensing, University of Chicago, Chicago, Illinois.
[2]Department of Biophysics, Medical College of Wisconsin, Milwaukee, Wisconsin.

importantly, our data further showed that selective scavenging of mitochondrial ROS prevents IH-induced sustained but not transient elevation of blood pressure in rats.

Materials and Methods

Exposure of cell cultures to IH

PC12 cells were cultured in Dulbecco's modified Eagle's medium (DMEM) supplemented with 10% horse serum, 5% fetal bovine serum (FBS), penicillin (100 U/mL), and streptomycin (100 μg/mL) under 10% CO_2 and 90% air (20% O_2) at 37°C. Before all experiments, the cells were serum starved for 16 h in antibiotic-free medium to avoid any confounding effects of serum. In the experiments involving treatment with drugs, cells were preincubated for 30 min with either drug or vehicle. Cell cultures were exposed to IH (1.5% O_2 for 30 s followed by 20% O_2 for 5 min at 37°C) as described previously (38, 39). O_2 levels were monitored by an electrode (Lazar) placed in the tissue culture medium and ambient O_2 levels were monitored by an O_2 analyzer (Beckman LB2).

Measurement of complex I activity

Complex I activity (NADH-ubiquinone reductase) was measured as rotenone (50 μM)-sensitive rate of NADH oxidation and expressed in nanomoles of NADH oxidized per min per mg protein as previously described (38). Protein analysis was performed using Bio-RAD protein assay kit.

siRNA studies

PC12 cells (5×10^5) were plated on collagen type IV (BD Biosciences)-coated culture dish and were grown for 24 h. The transfection was performed with siRNAs specific for Nox2, Nox4, or scrambled (control) sequences (Santa Cruz Biotechnology; Cat # sc-61838 (Nox2), sc-61887 (Nox4), and sc-37007 Scrambled; 100 pmol/mL) using a DharmaFECT-2 (Dharmacon Research) according to the manufacturer's recommendations. After transfection, cells were grown in the medium containing serum and antibiotics for 48 h before subjecting to either 60 cycles of IH or normoxia.

Measurement of NADPH oxidase activity

Membrane-enriched fractions from PC12 cells and brain were isolated as described (19). NADPH oxidase activity in the membrane-enriched protein fractions was measured using cytochrome *c* reduction assay as described (20). Briefly, the assay medium contained 100 μg membrane protein, cytochrome *c*, and NADPH at a final concentration of 150 and 100 μM, respectively, and 25 mM modified HEPES buffer (pH 7). The assay was performed in the presence and absence of superoxide dismutase (200 units/mL) at 37°C for 30 min. Cytochrome *c* reduction was measured by reading absorbance at 550 nm on a microplate reader. The amount of SOD inhibitable NADPH oxidase activity was calculated using extinction coefficient of 21 mmol/(L cm) and expressed in nmol/min/mg protein.

Measurement of aconitase activity

Mitochondrial fractions were isolated from cells or brain extracts by differential centrifugation as described (15). Aconitase enzyme activity was determined in the mitochondrial fractions as described (38) and expressed as nanomoles of isocitrate formed per minute per milligram of protein.

Measurement of S-glutathionylation

Cells were lysed in Mannitol/Tris/EDTA (MTE) buffer and mitochondrial fractions were isolated by differential centrifugation. The mitochondrial pellet was solubilized in 20 mM *N*-dodecyl-β-D-maltopyranoside (1% final concentration) and centrifuged at 72,000 *g* for 30 min. Immune complexes were precipitated from the supernatant using anticomplex I monoclonal antibody (Mitosciences, Eugene, OR) and Protein A/G agarose beads. Complexes were eluted from the beads using SDS buffer without mercaptoethanol and analyzed on 10% SDS-PAGE nonreducing gels and transferred to a polyvinylpyrrolidone difluoride membrane (Immobilon-P; Millipore). Membranes were incubated with antireduced form of glutathione (GSH) mouse monoclonal antibody (Virogen) at 1:1000 dilution of stock in Tris-buffered saline- Triton x-100 containing 3% nonfat milk after overnight blocking in 5% milk. Membranes were treated with goat anti-mouse secondary antibody conjugated with horseradish peroxidase (dilution 1:2,000; Chemicon) and immune complexes were observed using enhanced chemiluminescence (ECL) detection system (Amersham BioSciences). The membranes were exposed to Kodak XAR films.

Measurement of GSH and oxidized glutathione

GSH and oxidized glutathione levels were determined in PC12 cells using Glutathione assay kit (#703002; Cayman Chemicals). The sulfhydryl group of GSH reacts with DTNB (5,5′-dithio-bis-2-nitrobenzoic acid, Ellman's reagent) to produce a yellow-colored 5-thio-2-nitrobenzoic acid (TNB) product, the absorbance of which is measured at 405 nm. The rate of TNB production is directly proportional to the concentration of GSH. Quantification of oxidized from of glutathione (GSSG) exclusive of GSH is done by first derivatizing GSH with 2-vinylpyridine as described in the kit.

Exposure of mice and rats to IH and measurement of blood pressure

Experiments were approved by the Institutional Animal Care and Use Committee of the University of Chicago and were performed on adult male rats (200–300 g; Sprague Dawley), wild type (Wt, C57BL/6), hemizygous $gp91^{phox-/Y}$ (from Jackson Laboratories; weights 20–25 gm). Rats were treated with mito-tempol (10 mg/Kg; intraperitoneal [IP]), a selective scavenger of mitochondrial ROS or apocynin (10 mg/kg; IP) every day before 8 h regimen of IH treatment for 10 days. Unrestrained, freely moving animals housed in feeding cages were exposed to intermittent hypoxia for 10 days (IH; 8 h/day) as previously described (25–27). Briefly, animals were placed in a specialized chamber, which was flushed with alternating cycles of pure nitrogen and compressed air. During hypoxia, inspired O_2 levels reached 5% O_2 (nadir). The gas flows were regulated by timer-controlled solenoid valves. Ambient O_2 and CO_2 levels in the chamber were continuously monitored by an O_2/CO_2 analyzer (Series 9500; Alpha Omega Instrument). Control experiments were performed on animals exposed to alternating cycles of com-

pressed room air instead of hypoxia in the same chamber. Blood pressures were monitored by the tail cuff method in unanaesthetized rats using a noninvasive BP system (AD Instruments) as described (28). Rats were placed in the restrainer provided by the manufacturer and were allowed to acclimate for at least 1 h before blood pressure measurements. Baseline blood pressures were determined for 3 consecutive days in the morning (9 a.m.) and in the evening (5 p.m.). Subsequently, rats were exposed to IH for 10 days. Blood pressures were determined at the end 10th day within 1 and 15 h after terminating IH.

Chemicals

All chemicals were of analytical grade and obtained from commercial sources. Mito-tempol was prepared in the laboratories of Drs. Joseph and Kalyanaraman.

Data analysis

The data were expressed as mean ± SEM from at least three individual experiments. Two-way analysis of variance with repeated measures followed by Tukey's test was used to evaluate the statistical significance and p-values <0.05 were considered significant.

Results

Time course of IH on Nox and mitochondrial complex I activities

Nox and mitochondrial complex I activities were determined in PC12 cells treated with increasing durations of IH. Nox activity increased progressively in membrane fractions with increasing the duration of IH from 10, 30, and 60 cycles (Fig. 1A). Analysis of Nox activity using whole cell also revealed similar increase in response to IH (data not shown). Analysis of complex I activity in mitochondrial fractions showed progressive decrease with increasing the duration of IH (Fig. 1B). After re-oxygenation, Nox activity returned to baseline values within 3 h (Fig. 1A), whereas complex I activity remained downregulated significantly even after 24 h of re-oxygenation ($p < 0.05$; Fig. 1B).

Nox/ROS signaling mediates IH-evoked complex I inhibition

To assess whether Nox activation mediates IH-evoked complex I inhibition, PC12 cells were treated with two structurally distinct Nox inhibitors, apocynin (500 μM) or 4-(2-aminoethyl) benzenesulfonyl fluoride hydrochloride (300 μM). Cells treated with Nox inhibitors were challenged with 60 cycles of IH (*i.e.*, IH_{60}; the maximum duration of IH used in this study). Both Nox inhibitors prevented IH_{60}-evoked Nox activation and complex I inhibition (Fig. 2A, B).

Among the several isoforms of Nox (1), Nox2 mediates IH-evoked cellular responses in PC12 cells (39) and systemic responses in mice (27). The Nox inhibitors used in the above experiments cannot distinguish between different Nox isoforms. Therefore, siRNA approach was employed to assess the contribution of Nox 2 to IH-evoked complex I inhibition. Nox2 and Nox4 proteins were upregulated in IH-treated cells and this response was absent in cells transfected with Nox2 and Nox4 siRNAs (Fig. 2C; top panel). More importantly, IH-evoked inhibition of complex I activity was absent in cells treated with Nox2 but not Nox4 siRNA (Fig. 2C; bottom panel).

To further establish a role for Nox2 in IH-induced complex 1 inhibition, experiments were performed on age-matched wild-type (Wt) and hemizygous $gp91^{phox-/Y}$ mice (*i.e.*, Nox2 knock-out mice) treated with 10 days of IH, a duration chosen based on previous study (28). Nox and complex I activities were analyzed in brain stem samples from both groups of mice, We chose the brain stem region because it provides adequate amount of tissue for biochemical assays and neurons in this region mediate increased sympathetic tone, which is a hallmark of IH [reviewed in ref. (29)]. Nox activity was significantly elevated in IH-treated Wt mice but not in Nox2 KO mice (Fig. 2D). As in PC12 cells, mitochondrial complex I activity was inhibited in IH-treated Wt mice and remarkably this response was absent in Nox2 KO mice (Fig. 2E).

Ca^{2+} mediates IH-evoked complex I inhibition

Ca^{2+} inhibits mitochondrial complex I activity (32). IH activates Nox and the ensuing ROS elevates basal $[Ca^{2+}]_i$ levels

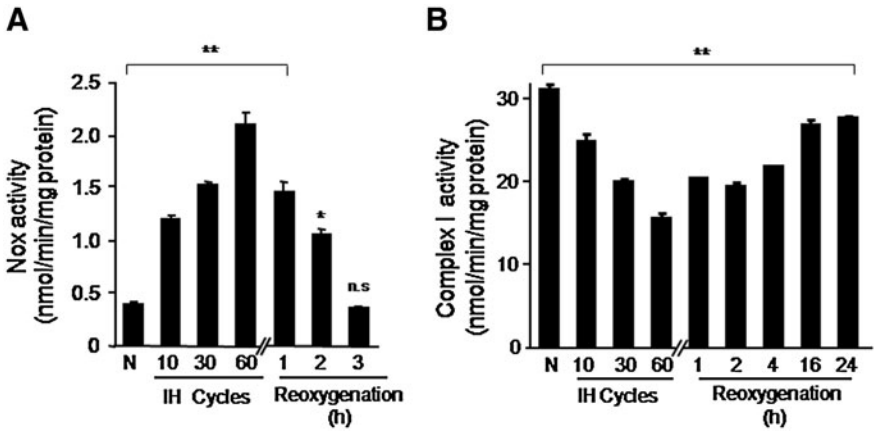

FIG. 1. Time course and reversibility of Nox and mitochondrial complex I activities during IH. (A) Nox activity was determined in membrane fractions of PC12 cells treated with increasing durations of IH. Reversibility of the response was determined by placing IH_{60}-treated cells under normoxia for varying periods. **(B)** Complex I activity was determined in mitochondrial fractions of PC12 cells treated with different durations of IH and after re-oxygenation. Data are mean ± SEM from four independent experiments run in triplicate. $^{**}p < 0.01$ and $^{*}p < 0.05$ compared to normoxic controls, respectively. IH_{60}, cells exposed to 60 cycles of intermittent hypoxia; N, normoxia; Nox, NADPH oxidase; n.s., not significant; PC12, pheochromocytoma 12.

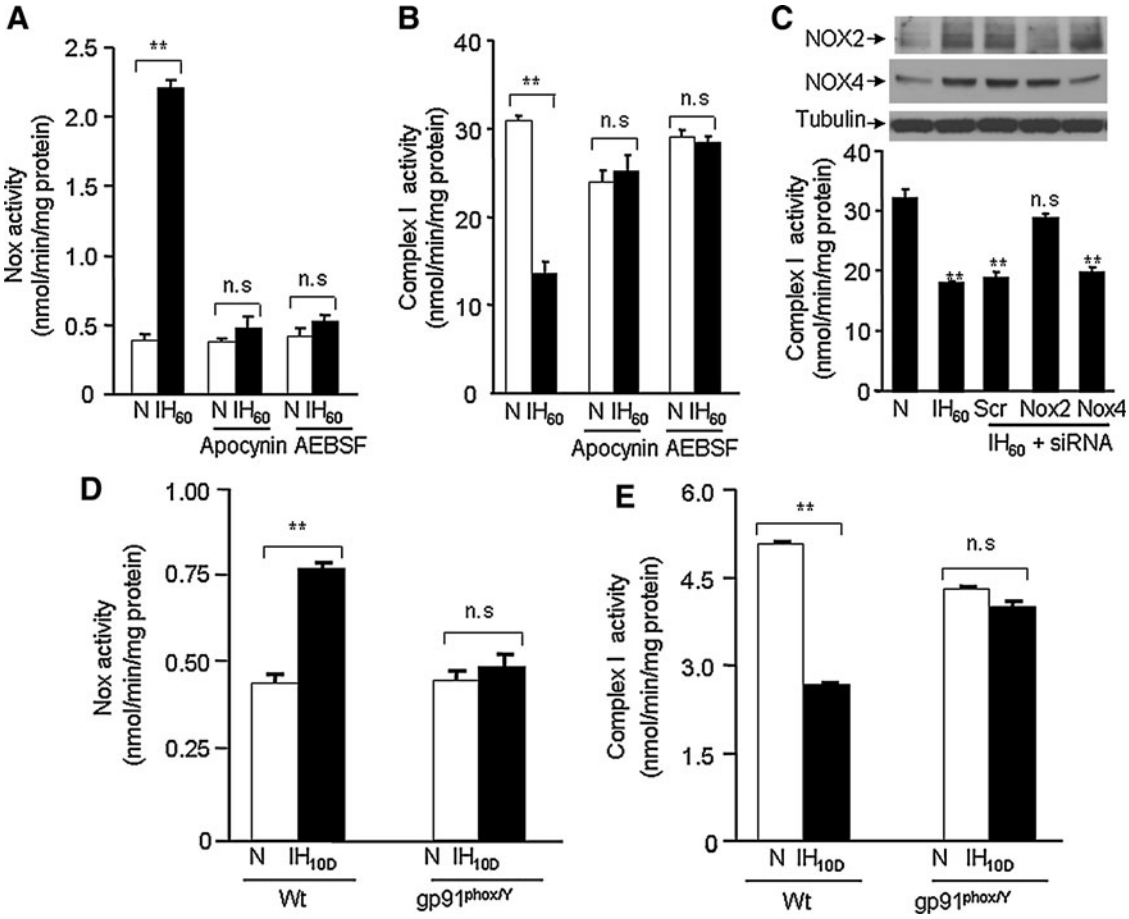

FIG. 2. Nox mediates IH-induced complex I inhibition. (A, B) Effects of two structurally distinct Nox inhibitors 500 μM apocynin or 300 μM AEBSF on Nox and complex I activities in IH_{60}-treated PC12 cells. **(C)** Effect of silencing Nox2 and Nox4 RNAs (siRNAs) on IH_{60}-evoked complex I inhibition. *Top panel* represents Western blots of Nox2 and Nox4 protein expressions in cells treated with normoxia (*lane 1*), IH_{60} (*lane 2*), IH+scr RNA (*lane 3*), IH_{60}+Nox2 siRNA (*lane 4*), and IH_{60}+Nox4 siRNA (*lane 5*). *Bottom panel* presents average data (mean ± SEM) of complex I activity. **(D, E)** Effect of 10 days of IH treatment (IH_{10D}) on Nox and complex I activities in brainstem tissue samples from wild-type and gp91 $^{phox-/Y}$ knock-out mice ($n = 5$ mice in each group). Data are mean ± SEM from three to five independent experiments. $^{**}p < 0.01$ compared to normoxic controls. AEBSF, 4-(2-aminoethyl) benzenesulfonyl fluoride hydrochloride; scr, scrambled; Wt, wild type.

in PC12 cells (39). We therefore reasoned that elevated cytosolic $[Ca^{2+}]_i$ and the resulting Ca^{2+} entry into mitochondria inhibits complex I. To test this possibility, cells were treated with increasing concentrations (1, 3, and 10 μM) of 1,2-bis(o-aminophenoxy)ethane-*N*,*N*,*N*′,*N*′-tetraacetic acid (BAPTA-AM), an intracellular Ca^{2+}-chelator, and as shown in Figure 3A, 10 μM BAPTA-AM completely prevented IH-induced complex I inhibition. Likewise, 10 μM ruthenium red (RR) an inhibitor of mitochondrial Ca^{2+} uniporter, which mediates Ca^{2+}entry into mitochondria, also prevented complex I inhibition in IH_{60}-treated cells (Fig. 3A). Treating control cells with Ca^{2+} ionophore (1.4 μM ionomycin) inhibited the complex I activity, and 10 μM RR or BAPTA-AM prevented this effect (Fig. 3B).

To further assess the effects of Ca^{2+}, complex I activity was determined in the presence of varying concentrations of Ca^{2+}. Increasing the concentration of Ca^{2+} from 0–80 μM progressively inhibited complex I activity in control cells with a K_i of $5.3 + 0.4$ μM and this effect was not seen in IH-treated cells (Fig. 4A). Analysis of complex I activity as a function of NADH concentration in the presence of 20 μM Ca^{2+} (4xKi) revealed a ~2-fold reduction in V_{max} and K_m (Fig. 4B). The baseline V_{max} and K_m values in IH_{60}-treated cells were significantly lower than control cells but quite similar to those in Ca^{2+}-treated control cells (V_{max}: $IH_{60} = 20.92 \pm 0.14$ *vs.* Control+20 μM $Ca^{2+} = 23.32 \pm 0.20$ nmol/min/mg; K_m: IH_{60} 59.24 ± 3.68 *vs.* Control+20 μM $Ca^{2+} = 69.50 \pm 2.02$ μM). Addition of 20 μM Ca^{2+} had no further effect on either V_{max} or K_m in IH_{60}-treated cells (Fig. 4C).

IH increases S-glutathionylation of mitochondrial complex I subunits

Ca^{2+}-induced inhibition of the complex I activity can be reversed by sulfhydryl reducing agents, suggesting that oxidative modification of sulfhydryl residues leads to inhibition of complex I (34). S-glutathionylation of 75-kDa protein of complex I subunit represents one such sulfhydryl modification reaction (12). We monitored S-glutathionylation of 75-kDa and ~50 kDa complex I proteins in control and IH_{60}-treated cells. Mitochondrial complex I proteins were immunoprecipitated and probed with anti-glutathione antibody.

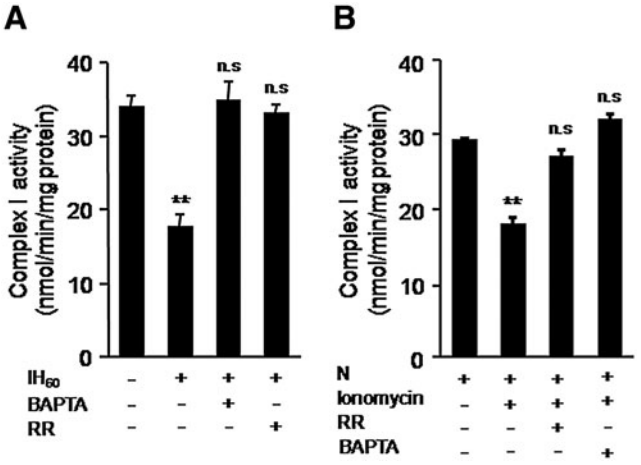

FIG. 3. Ca^{2+} is required for IH-evoked complex 1 inhibition. (A) Effect of Ca^{2+} chelator BAPTA-AM (10 μM BAPTA) and RR, an inhibitor Ca^{2+} uniporter (10 μM) on complex I activity in IH_{60}-treated PC12 cells. **(B)** Effect of ionomycin (1.4 μM), a Ca^{2+} ionophore on complex I activity in normoxic PC 12 cells with and without RR. $^{**}p < 0.01$ compared to controls; BAPTA, 1,2-bis(o-aminophenoxy)ethane-*N*,*N*,*N*′,*N*′-tetraacetic acid; RR, ruthenium red.

S-glutathionylation of 75- and 50-kDa subunits of complex I increased by 2.5- and 3.5-fold, respectively, in IH_{60}-treated cells compared with control cells (Fig. 5A; panel 1). Similar increases in S-glutathionylation of complex I subunits were also seen in control cells challenged with a Ca^{2+} ionophore (1.4 μM ionomycin) (Fig. 5A, panel 2). RR (10 μM) prevented the increase in S-glutathionylation of complex I subunits in IH_{60} as well as ionomycin-treated control cells (Fig. 5A, panels 1 and 2).

IH-evoked S-glutathionylation of complex I subunits was absent in PC12 cells treated with 500 μM apocynin or manganese(III) tetrakis(1-methyl-4-pyridyl)porphyrin, a ROS scavenger or transfected with Nox2 siRNA (Fig. 5A; panels 3 and 4). Further, IH treatment also increased S-glutathionylation of mitochondrial complex I subunits in brain stem tissues from Wt mice and this effect was absent in tissues from Nox2 KO mice (Fig. 5A, panel 5). In addition, treatment of cells with *N*-acetyl-cysteine, a precursor of glutathione, also prevented IH-induced S-glutahtionylation of complex I subunits (Fig. 5A, panel 6).

Glutathione prevents IH-induced complex I inhibition

S-glutathionylation requires oxidation of glutathione to glutathione disulfide (GSSG). Therefore, we determined whether IH affects the ratio of GSSG/GSH and whether addition of GSH reverses the inhibition of complex I activity in IH_{60}-treated cells. As shown in Figure 5B, ratio of GSSG/GSH increased by ~2-fold in IH_{60}-treated cells compared with controls. Addition of GSH to mitochondrial fractions from IH_{60} cells restored the complex I activity in a concentration-dependent manner with a complete recovery occurring at 5 mM GSH (Fig. 5C). Since oxidative modification of sulfhydryl residues leads to inhibition of complex I, reducing agents like dithiothreitol (DTT) should prevent IH-induced complex 1 inhibition. Indeed, treatment of cells with 1 mM DTT prevented inhibition of complex I by IH (Fig. 5D).

Analysis of the complex I activity as a function of NADH in the presence and absence of 5 mM GSH showed that GSH increased the V_{max} of the reaction by 65% in IH_{60}-treated cells, whereas it did not alter V_{max} in the control cells (Fig. 6A, B). On the other hand, GSH did not affect the K_m of NADH both in the control as well as IH_{60}-treated cells (Fig. 6A, B).

IH-induced complex I inhibition increases mitochondrial ROS

We determined whether IH-evoked complex I inhibition increases ROS generation in the mitochondria. The aconitase

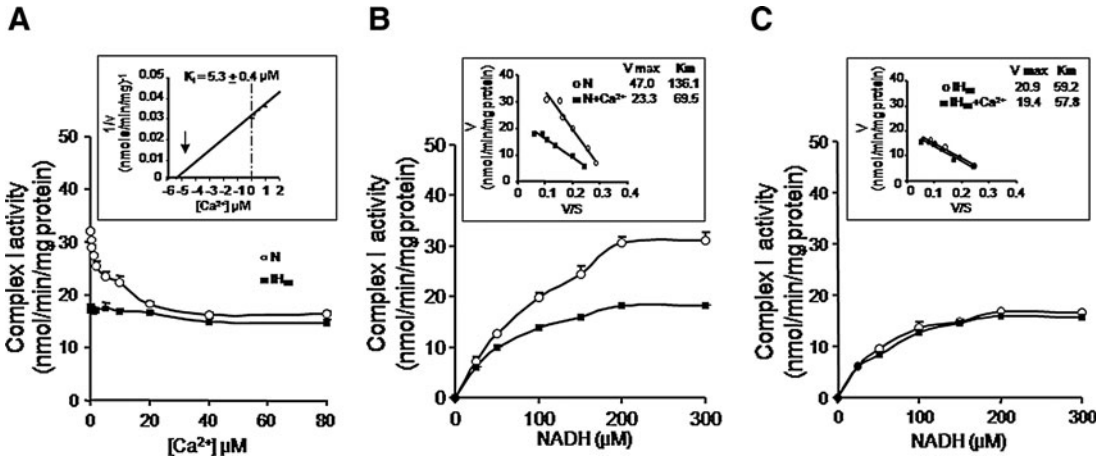

FIG. 4. Kinetic analysis of the effects of Ca^{2+} on complex I activity. (A) Increasing Ca^{2+} concentrations inhibited complex I activity in control PC 12 cells (o-o) but not in IH exposed cells (■-■) (*inset*: plot of the reciprocal of complex I activity (1/V) *versus* Ca^{2+} concentration. Intercept represents the concentration required to produce 50% inhibition of the enzyme, that is, Ki. **(B, C)** Mitochondrial fractions were assayed for complex 1 activity with increasing NADH concentrations (0–300 μM) in control (N) and IH_{60}-treated cells in the absence (o-o) or presence (■-■) of 20 μM Ca^{2+}. *Inset* represents the Eadie-Hofstee plot of rate (V) *versus* V/S (S is the NADH concentration). V_{max} and K_m were calculated from the intercept and slope, respectively. Each data point represents the mean ± SEM from three independent experiments.

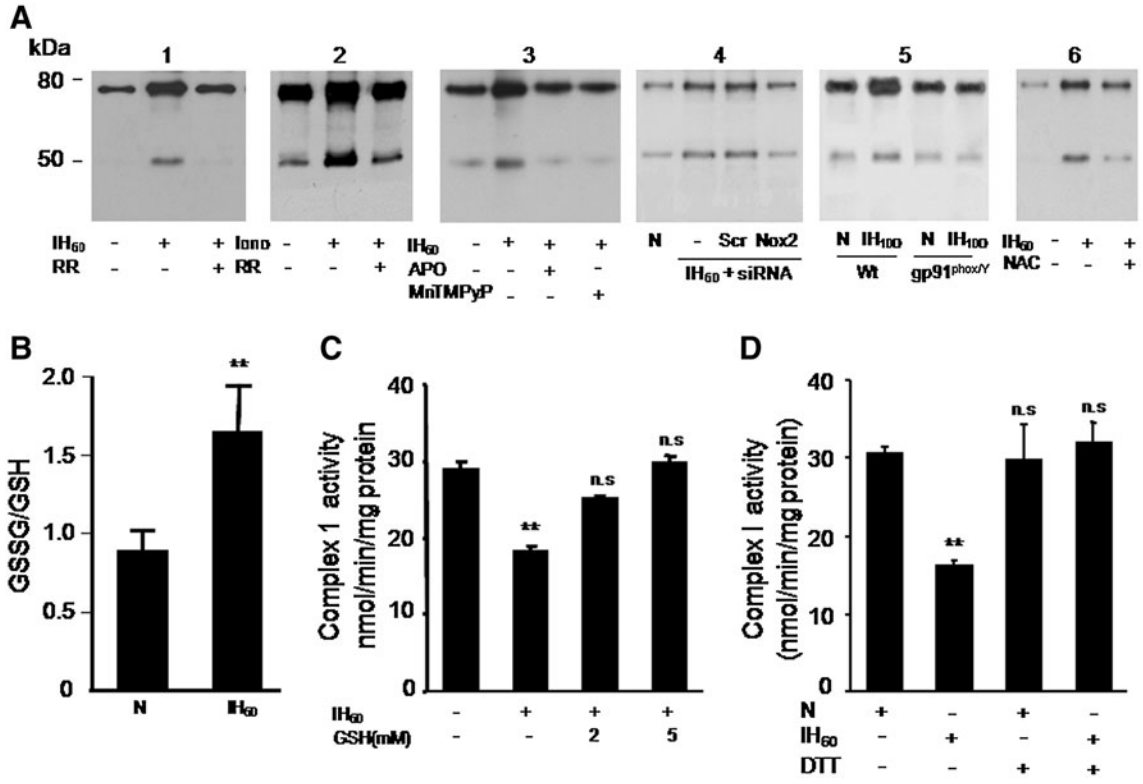

FIG. 5. IH increases S-glutathionylation of mitochondrial complex I subunits. (A) Representative immunoblots showing increased S-glutathionylation of 75- and 55-kDa subunits of the complex I in IH_{60} and ionomycin (Iono; 1.4 μM)-treated PC12 cells and blockade of the responses by RR (10 μM; *panels 1* and *2*). Blockade of IH_{60}-induced S-glutathionylation of complex I subunits by Nox inhibitor apocynin (Apo; 500 μM) and antioxidant (MnTMPyP; 50 μM; *panel 3*) and by Nox2 siRNA (*panel 4*). S-glutathionylation of complex I subunits in brain stem cell lysates from wild-type (Wt) and gp91phox-/Y mice treated with either 10 days of normoxia or IH (*panel 5*). Note the absence of increased S-glutathionylation of complex I subunits in tissues lysates from IH-treated $gp91^{phox-/Y}$ mice. Blockade of IH_{60}-induced S-glutathionylation of complex I subunits by *N*-acetyl-cysteine (2 mM NAC), a precursor of glutathione (*panel 6*). **(B)** Ratio of oxidized from of glutathione/GSH was determined in normoxic (N) and IH_{60}-treated PC12 cells as described in Materials and Methods. **(C)** IH-induced inhibition of complex I activity is prevented in the presence of 2 and 5 mM GSH or **(D)** 2 μM dithiothreitol (DTT). Data represent the mean $\pm$ SEM from three to five independent experiments $^{**}p < 0.01$ compared to normoxic controls (N). GSH, reduced form of glutathione; MnTMPyP, manganese(III) tetrakis(1-methyl-4-pyridyl)porphyrin; NAC, *N*-acetyl-cysteine.

enzyme activity was monitored in the mitochondrial fractions as an index of ROS generation (10). Mitochondrial aconitase activity progressively decreased as the duration of IH increased from 10 to 60 cycles and remained significantly inhibited even after 24 h of re-oxygenation (Fig. 7A). IH-evoked inhibition of aconitase activity was prevented by Nox inhibitor (apocynin), Ca^{2+}chelator (BAPTA-AM), RR, an inhibitor of mitochondrial Ca^{2+} uniporter, as well as by *N*-acetyl-cysteine, a precursor of GSH and by manganese(III) tetrakis(1-methyl-4-pyridyl)porphyrin, an antioxidant (Fig. 7B). Further, inhibition of mitochondrial aconitase activity was absent in cells transfected with Nox2 but not with Nox4 or scrambled siRNAs (Fig. 7C).

Mitochondrial ROS contributes to IH-induced sustained elevation in blood pressure

Previous studies reported that antioxidant treatment prevents IH-evoked hypertension in rodents [reviewed in refs. (29, 35)], suggesting a role for ROS signaling. To address the role of ROS generated by Nox and mitochondria in IH-evoked hypertension, rats were treated with apocynin (10 mg/Kg; IP), a Nox inhibitor or mito-tempol (10 mg/Kg; IP), a selective scavenger of mitochondrial ROS (21) each day before 8 h regimen of IH treatment for 10 days. Blood pressures were monitored $\sim$1 and $\sim$15 h after terminating the IH regimen in unsedated rats. The results are summarized in Figure 8A. In vehicle-treated IH rats, mean blood pressures were elevated measured after $\sim$1 as well as $\sim$15 h after terminating IH. Mito-tempol treatment abolished sustained elevations in blood pressures measured at $\sim$15 h without affecting the blood pressure elevations seen within 1 h after terminating IH. In contrast, apocynin treatment prevented both early (within 1 h) and sustained (after 15 h) elevations in blood pressure (Fig. 8A). Results similar to apocynin treatment were also obtained in Nox-2 KO mice (data not shown).

Mitochondrial aconitase and Nox activities were determined in brain stem samples from rats treated with IH alone or in combination with mito-tempol or apocynin. In mito-tempol-treated rats IH-evoked decreases in mitochondrial aconitase activity (index of ROS) and complex I activities were

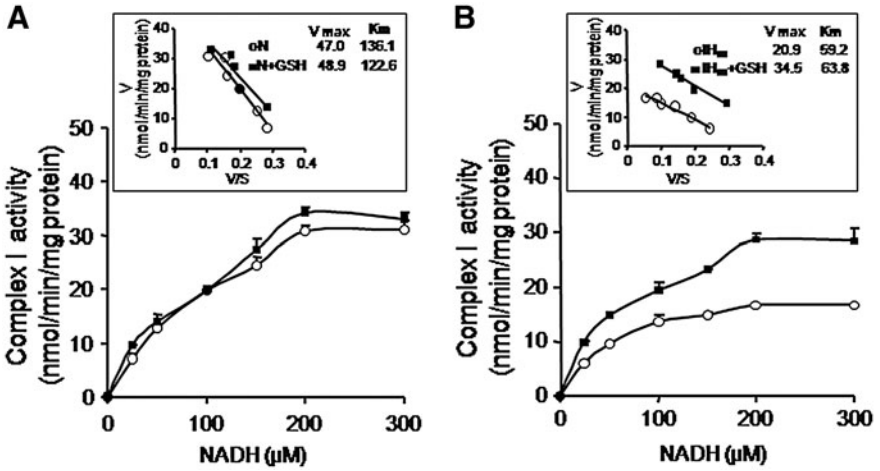

FIG. 6. GSH prevents IH-evoked complex I inhibition by restoring V_{max}. Complex I activity was determined as a function of NADH concentration with (■-■) and without (o-o) addition of 5 mM GSH in control (N) (**A**) and IH_{60}-treated PC12 cells (**B**). *Insets* represent Eadie-Hofstee plots of rate (V) *versus* V/S (S is the NADH concentration). V_{max} and K_m are calculated from the intercept and slope, respectively.

absent, whereas increased Nox activity was unaffected (Fig. 8B–D). On the other hand, apocynin treatment prevented IH-evoked decrease in mitochondrial aconitase and complex I activities as well as increased Nox activity (Fig. 8B–D).

Discussion

The present study reveals three novel and mechanistically linked findings: (i) IH-evoked mitochondrial complex I inhibition requires ROS generation by Nox2 and S-glutathionylation of complex I subunits, (ii) inhibition of complex I increases mitochondrial ROS, and (iii) mitochondrial ROS contributes to sustained but not transient elevations in blood pressure in IH-treated rats.

We previously reported that IH activates Nox (26) and inhibits mitochondrial complex I activity (27) in the rat carotid body. However, carotid bodies being too small in size (weighing 50–80 μg) precluded analysis of potential interactions between Nox and complex I. PC12 cells respond similarly to IH with increased Nox and decreased mitochondrial complex I activities (38, 39) (Fig. 1), which prompted us to assess the interactions between Nox and mitochondrial complex I in this cell line. We further verified the data from PC12 cell cultures with brain stem tissue from intact mice or rats and found that IH increased Nox and decreased complex I activities in both preparations. However, Nox activity measured in brainstem tissue was lower than in PC12 cells. It is likely that Nox is expressed in certain population of neurons or a subset of glial cells, whereas PC12 cells are a homogenous population. The heterogeneity of brain stem tissue might account for the relatively lower complex I and Nox activities compared to PC12 cell cultures. Further, we also found similar changes in Nox and complex 1 activity in cerebral cortical tissue samples from IH-treated rats and mice, suggesting that these responses can be seen in other neural tissues as well.

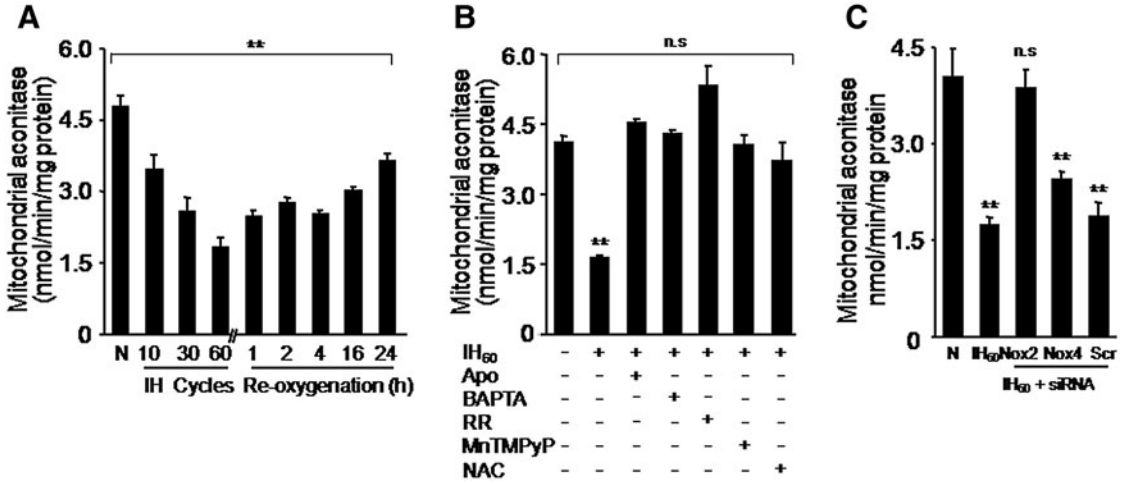

FIG. 7. IH increases mitochondrial ROS. Mitochondrial aconitase activity was determined as index of ROS. (**A**) Aconitase activity in the mitochondrial fractions from PC12 cells treated with normoxia (N) or to increasing durations of IH as indicated (IH cycles). For reversibility studies, PC12 cells exposed to IH_{60} were placed in normoxia for indicated duration (h). (**B**) Effect of apocynin (500 μM), BAPTA (10 μm), RR (10 μm), and MnTMPyP (50 μM), NAC (500 μM) on mitochondrial aconitase activity in IH_{60}-treated PC12 cells. (**C**) IH-induced inhibition of mitochondrial aconitase activity was absent in PC12 cells transfected with Nox2 siRNA but not with Nox4 siRNA or scr RNAs. Data are mean ± SEM from three to four independent experiments. $^{**}p < 0.01$ compared to normoxia. ROS, reactive oxygen species.

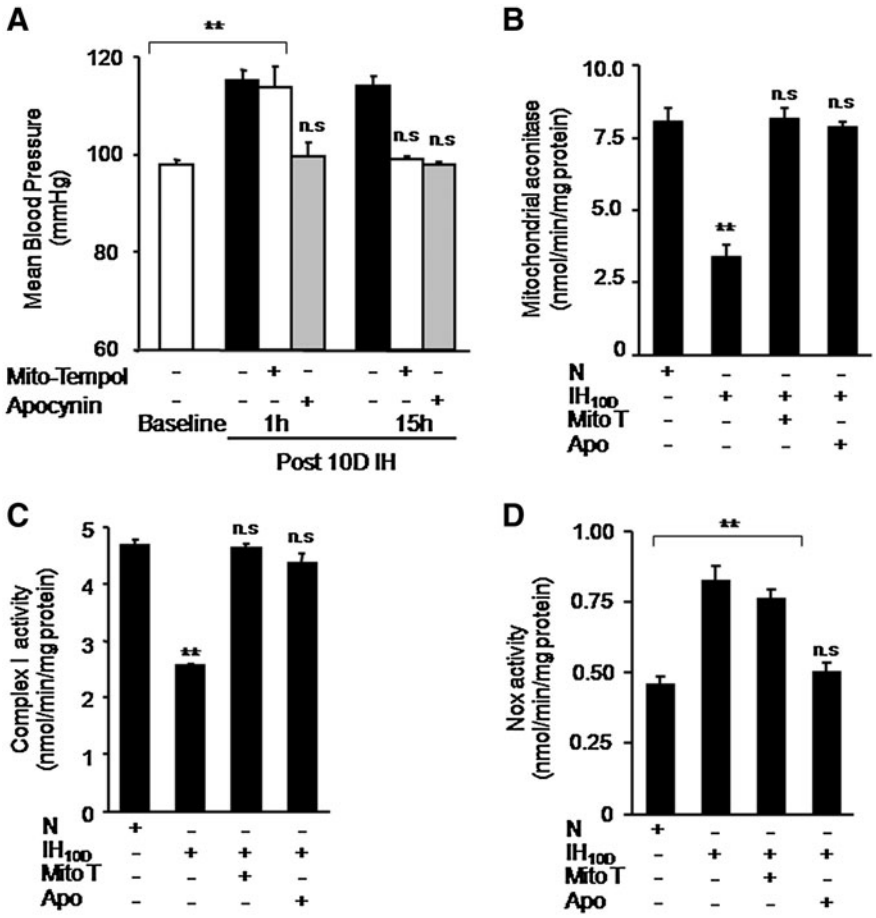

FIG. 8. Effects of systemic administration of mitochondrial ROS scavenger mito-tempol or apocynin, a Nox inhibitor on blood pressure, mitochondrial aconitase, and NOX activity in rats exposed to 10 days IH. Adult rats were exposed to 10 days of IH and were treated daily with either saline (IH) or mito-tempol (10 mg/kg/day; intraperitoneal) or apocynin (10 mg/kg/day; intraperitoneal). Control experiments were performed on rats exposed to normoxia (N). (**A**) Mean blood pressure values measured ~1 and ~15 h after terminating 10 days of IH with and without mito-tempol or apocynin treatment. (**B, C**) Treatments with mito-tempol or apocynin prevented IH-induced decrease in mitochondrial aconitase and complex 1 activities. (**D**) IH-evoked increase in Nox activity was unaffected by mito-tempol but prevented by apocynin treatment. Data presented are mean ± SEM from six rats in each group. $^{**}p < 0.01$.

The following observations demonstrate that activation of Nox, especially Nox2 by IH, mediates complex I inhibition: (a) two structurally distinct inhibitors of Nox prevented IH-evoked inhibition of complex I; (b) genetic silencing of Nox2 but not Nox 4 abrogated complex I inhibition in IH-treated cells, and (c) complex I inhibition by IH was absent in tissues from Nox2 KO mice. Consistent with previous studies (3, 5, 7, 13) we found that activation of Nox increases mitochondrial ROS. It has been proposed that mitochondrial permeability transition pore (mPTP) plays a critical role in mitochondrial redox signaling (6, 11, 21). The possibility that IH-induced mitochondrial ROS might be due to changes in mPTP requires further investigation. The finding that Nox activation by IH causes mitochondrial complex I inhibition under IH is reminiscent of mitochondrial dysfunction by Nox activation by angiotensin (37) and nitoglycerine (36). Nox activation by IH was transient and reversible, whereas complex I inhibition was long lasting. It is likely that transient Nox activation by IH and the ensuing ROS triggers prolonged ROS generation by mitochondria *via* inhibition of complex I activity. In other words, these data indicate that IH evokes ROS-induced ROS mechanism. Taken together these observations demonstrate a functional cross-talk between Nox and mitochondrial complex I activity under IH leading to mitochondrial dysfunction. Whether increased mitochondrial ROS impacts Nox activation as proposed recently (16, 31) also plays a role in IH remain to be investigated.

Our results provide further insight into how Nox activation by IH inhibits complex I. Yuan *et al.* (39) reported that ROS generated by Nox leads to persistent elevation of baseline $[Ca^{2+}]_i$ in IH-treated PC12 cells. The following observations demonstrate that Ca^{2+} is critical for evoking complex I inhibition in IH-treated cells: (a) BAPTA-AM, a Ca^{2+} chelator or RR, an inhibitor of mitochondrial Ca^{2+} uniporter prevented IH-evoked complex I inhibition; (b) ionomycin, a Ca^{2+} ionophore inhibited complex I activity in control cells and this effect was prevented by RR; and (c) Ca^{2+} inhibited the complex I activity in control cells, and this effect was occluded in IH-treated cells. It can be argued that RR may inhibit Ca^{2+} release from the sarcoplasmic reticulum as evidenced in normal cardiomyocytes (4). However, RR at the concentrations that prevented complex I inhibition in IH-treated cells had no impact on complex I activity in control PC12 cells. Taken together, these observations suggest that Ca^{2+} entry into mitochondria is critical for complex I inhibition in IH-treated cells.

How might Ca^{2+} inhibit the mitochondrial complex I activity? Previous studies identified two catalytically distinct forms of mitochondrial complex I, including an active A-form and the other deactivated D-form (8). Ca^{2+} and other divalent cations facilitate the transition of active-to-deactivated form of the complex I with altered substrate affinity (9). IH decreased the substrate affinity of the complex I similar to that seen in control cells treated with Ca^{2+}, suggesting that IH causes Ca^{2+}-dependent conformational change in complex I similar to that reported with ischemia and re-perfusion in rat heart preparation (32). Previous studies have shown that the deactivated, not the active, form of the complex I is susceptible to redox modifications (8). Indeed IH caused redox modulation

of modification of complex I as evidenced by increased S-glutathionylation of 75 and 50 kDa subunits both in cell cultures and in the brain tissues from IH-treated mice. The findings that IH-evoked S-glutathionylation can be blocked by a Ca^{2+}chelator as well as RR and mimicked by a Ca^{2+} ionophore further support the notion that IH-induced S-glutationylation involves a Ca^{2+}-dependent conformational change of complex I subunits.

S-glutathionylation, in addition to conformational change of the complex I, also requires elevated GSSG levels (2). Not only did IH elevate GSSG as evidenced by increased ratio of GSSG/GSH, but more importantly, addition of GSH (reduced form) abrogated complex I inhibition and restored the V_{max} of the reaction in IH-treated cells. These results demonstrate that S-glutathionylation is the critical signaling event responsible for IH-evoked complex I inhibition. The findings that IH-evoked S-glutathionylation could be prevented by a Nox inhibitor as well as by genetic silencing of Nox 2 in cell cultures and was absent in IH-treated Nox2 KO mice suggest that Nox 2 activation by IH and the resulting ROS mediate S-glutathionylation.

IH increased mitochondrial ROS, as evidenced by decreased mitochondrial aconitase activity, an *in vivo* marker of ROS. This increase in mitochondrial ROS was due to complex I inhibition, because preventing complex I inhibition abrogated the changes in mitochondrial aconitase activity. What might be the physiological significance of increased mitochondrial ROS by IH? One of the hallmarks of IH is the elevated blood pressures [reviewed in (29) and the present study]. Although ROS signaling has been implicated in IH-induced hypertension (28, 35), the relative importance of mitochondrial ROS has not been established. Our results showed that treatment with mito-tempol, a mitochondrial ROS scavenger, selectively abolished sustained but not the acute elevations of blood pressure in IH-treated rats, suggesting a role for mitochondrial ROS in IH-evoked hypertension. On the other hand, Nox inhibition by apocynin prevented both the transient as well as sustained elevations in blood pressures. Although cellular mechanisms by which mitochondrial ROS contribute to sustained elevations in blood pressure in IH-treated rats remain to be investigated, our results suggest a role for mitochondrial ROS generated by complex I inhibition resulting from Nox activation in mediating IH-induced long-lasting elevations of blood pressures.

Acknowledgments

This work was supported by National Institutes of Health–National, Heart, Lung, and Blood Institute Grants HL-90554, HL-76537, and HL-86493.

Author Disclosure Statement

No competing financial interests exist.

References

1. Bedard K and Krause KH. The NOX family of ROS-generating NADPH oxidases: physiology and pathophysiology. *Physiol Rev* 87: 245–313, 2007.
2. Beer SM, Taylor ER, Brown SE, Dahm CC, Costa NJ, Runswick MJ, and Murphy MP. Glutaredoxin 2 catalyzes the reversible oxidation and glutathionylation of mitochondrial membrane thiol proteins: implications for mitochondrial redox regulation and antioxidant defense. *J Biol Chem* 279: 47939–47951, 2004.
3. Brandes RP. Triggering mitochondrial radical release: a new function for NADPH oxidases. *Hypertension* 45: 847–848, 2005.
4. Corbalan-Garcia S, Teruel JA, and Gomez-Fernandez JC. Characterization of ruthenium red-binding sites of the $Ca^{(2+)}$-ATPase from sarcoplasmic reticulum and their interaction with $Ca^{(2+)}$-binding sites. *Biochem J* 287: 767–774, 1992.
5. Daiber A. Redox signaling (cross-talk) from and to mitochondria involves mitochondrial pores and reactive oxygen species. *Biochim Biophys Acta* 1797: 897–906, 2010.
6. Di Lisa F and Bernardi P. Mitochondria and ischemia-reperfusion injury of the heart: fixing a hole. *Cardiovasc Res* 70: 191–199, 2006.
7. Doughan AK, Harrison DG, and Dikalov SI. Molecular mechanisms of angiotensin II-mediated mitochondrial dysfunction: linking mitochondrial oxidative damage and vascular endothelial dysfunction. *Circ Res* 102, 488–496, 2008.
8. Galkin A and Moncada S. S-nitrosation of mitochondrial complex I depends on its structural conformation. *J Biol Chem* 282: 37448–37453, 2007.
9. Galkin A, Abramov AY, Frakich N, Duchen MR, and Moncada S. Lack of oxygen deactivates mitochondrial complex I: implications for ischemic injury? *J Biol Chem* 284: 36055–36061, 2009.
10. Gardner PR, Raineri I, Epstein LB, and White CW. Superoxide radical and iron modulate aconitase activity in mammalian cells. *J Biol Chem* 270: 13399–13405, 1995.
11. Hausenloy D, Wynne A, Duchen M, and Yellon D. Transient mitochondrial permeability transition pore opening mediates preconditioning-induced protection. *Circulation* 109: 1714–1717, 2004.
12. Hurd TR, Requejo R, Filipovska A, Brown S, Prime TA, Robinson AJ, Fearnley IM, and Murphy MP. Complex I within oxidatively stressed bovine heart mitochondria is glutathionylated on Cys-531 and Cys-704 of the 75-kDa subunit: potential role of cys residues in decreasing oxidative damage. *J Biol Chem* 283: 24801–24815, 2008.
13. Kimura S, Zhang G, Nishiyama A, Shokoji T, Yao L, Fan Y, Rahman M, Suzuki T, Maeta H, and Abe Y. Role of NAD(P)H oxidase- and mitochondria-derived reactive oxygen species in cardioprotection of ischemic reperfusion injury by angiotensin II. *Hypertension* 45, 860–866, 2005.
14. Kuri BA, Khan SA, Chan SA, Prabhakar NR, and Smith CB. Increased secretory capacity of mouse adrenal chromaffin cells by chronic intermittent hypoxia: involvement of protein kinase C. *J Physiol* 584: 313–319, 2007.
15. Lai JC and Clark JB. Preparation of synaptic and non-synaptic mitochondria from mammalian brain. *Meth Enzymol* 55: 51–60, 1979.
16. Lee SB, Bae IH, Bae YS, and Um HD. Link between mitochondria and NADPH oxidase 1 isozyme for the sustained production of reactive oxygen species and cell death. *J Biol Chem* 281, 36228–36235, 2006.
17. Lenaz G. The mitochondrial production of reactive oxygen species: mechanisms and implications in human pathology. *IUBMB Life* 52: 159–164, 2001.
18. Leto TL, Morand S, Hurt D, and Ueyama T. Targeting and regulation of reactive oxygen species generation by Nox family NADPH oxidases. *Antioxid Redox Signal* 11: 2607–2619, 2009.
19. Li JM and Shah AM. Intracellular localization and preassembly of the NADPH oxidase complex in cultured endothelial cells. *J Biol Chem* 277: 19952–19960, 2002.

20. Li JM, Mullen AM, and Shah AM. Phenotypic properties and charecteristics of superoxide production by mouse coronary microvascular endothelial cells. *J Mol Cell Cardiol* 33: 1119–1131, 2001.
21. Lim SY, Davidson DJ, Hausenloy DJ, and Yellon DM. Preconditioning and postconditioning: the essential role of the mitochondrial permeability transition pore. *Cardivasc Res* 75: 530–535, 2007
22. MacFarlane PM, Satriotomo I, Windelborn JA, and Mitchell GS. NADPH oxidase activity is necessary for acute intermittent hypoxia-induced phrenic long-term facilitation. *J Physiol* 587: 1931–1942, 2009.
23. Murphy MP. How mitochondria produce reactive oxygen species. *Biochem J* 417: 1–13, 2009.
24. Nieto FJ, Young TB, Lind BK, Shahar E, Samet JM, Redline S, D'Agostino RB, Newman AB, Lebowitz MD, and Pickering TG. Association of sleep-disordered breathing, sleep apnea, and hypertension in a large community-based study. Sleep Heart Health Study. *JAMA* 283: 1829–1836, 2000.
25. Peng YJ and Prabhakar NR. Reactive oxygen species in the plasticity of respiratory behavior elicited by chronic intermittent hypoxia. *J Appl Physiol* 94: 2342–2349, 2003.
26. Peng YJ, Nanduri J, Yuan G, Wang N, Deneris E, Pendyala S, Natarajan V, Kumar GK, and Prabhakar NR. NADPH oxidase is required for the sensory plasticity of the carotid body by chronic intermittent hypoxia. *J Neurosci* 29: 4903–4910, 2009.
27. Peng YJ, Overholt JL, Kline D, Kumar GK, and Prabhakar NR. Induction of sensory long-term facilitation in the carotid body by intermittent hypoxia: implications for recurrent apneas. *Proc Natl Acad Sci USA* 100: 10073–10078, 2003.
28. Peng YJ, Yuan G, Ramakrishnan D, Sharma SD, Bosch-Marce M, Kumar GK, Semenza GL, and Prabhakar NR. Heterozygous HIF-1alpha deficiency impairs carotid body-mediated systemic responses and reactive oxygen species generation in mice exposed to intermittent hypoxia. *J Physiol* 577: 705–716, 2006.
29. Prabhakar NR, Kumar GK, Nanduri J, and Semenza GL. ROS signaling in systemic and cellular responses to chronic intermittent hypoxia. *Antioxid Redox Signal* 9: 1397–1403, 2007.
30. Prabhakar NR, Peng YJ, Kumar GK, and Pawar A. Altered carotid body function by intermittent hypoxia in neonates and adults: relevance to recurrent apneas. *Respir Physiol Neurobiol* 157: 148–153, 2007.
31. Rathore R, Zheng YM, Niu CF, Liu QH, Korde A, Ho YS, and Wang YX. Hypoxia activates NADPH oxidase to increase [ROS]i and [Ca^{2+}]i through the mitochondrial ROS-PKCepsilon signaling axis in pulmonary artery smooth muscle cells. *Free Radic Biol Med* 45, 1223–1231, 2008.
32. Sadek HA, Szweda PA, and Szweda LI. Modulation of mitochondrial complex I activity by reversible Ca^{2+} and NADH mediated superoxide anion dependent inhibition. *Biochemistry* 43: 8494–8502, 2004.
33. Souvannakitti D, Kumar GK, Fox A, and Prabhakar NR. Neonatal intermittent hypoxia leads to long-lasting facilitation of acute hypoxia-evoked catecholamine secretion from rat chromaffin cells. *J Neurophysiol* 101: 2837–2846, 2009.
34. Sriram K, Shankar SK, Boyd MR, and Ravindranath V. Thiol oxidation and loss of mitochondrial complex I precede excitatory amino acid-mediated neurodegeneration. *J Neurosci* 18**:** 10287–10296, 1998.
35. Troncoso Brindeiro CM, Silva AQ, Allahdadi KJ, Youngblood V, and Kanagy NL. Reactive oxygen species contribute to sleep apnea-induced hypertension in rats. *Am J Physiol Heart Circ Physiol* 293: H2971–H2976, 2007.
36. Wenzel P, Mollnau H, Oelze M, Schulz E, Wickramanayake JM, Müller J, Schuhmacher S, Hortmann M, Baldus S, Gori T, Brandes RP, Münzel T, and Daiber A. First evidence for a crosstalk between mitochondrial and NADPH oxidase-derived reactive oxygen species in nitroglycerin-triggered vascular dysfunction. *Antioxid Redox Signal* 10, 1435–1447, 2008.
37. Wosniak J Jr., Santos CX, Kowaltowski AJ, and Laurindo FR. Cross-talk between mitochondria and NADPH oxidase: effects of mild mitochondrial dysfunction on angiotensin II-mediated increase in Nox isoform expression and activity in vascular smooth muscle cells. *Antioxid Redox Signal* 11, 1265–1278, 2009.
38. Yuan G, Adhikary G, McCornick AA, Holcroft JJ, Kumar GK, and Prabhakar NR. Role of oxidative stress in intermittent hypoxia-induced immediate early gene activation in rat PC12 cells. *J Physiol* 557: 773–783, 2004.
39. Yuan G, Nanduri J, Khan S, Semenza GL, and Prabhakar NR. Induction of HIF-1α expression by intermittent hypoxia: involvement of NADPH oxidase, Ca^{2+}signaling, prolyl hydroxylases, and mTOR. *J Cell Physiol* 217: 674–685, 2008.
40. Zhan G, Serrano F, Fenik P, Hsu R, Kong L, Pratico D, Klann E, and Veasey SC. NADPH oxidase mediates hypersomnolence and brain oxidative injury in a murine model of sleep apnea. *Am J Respir Crit Care Med* 172: 921–929, 2005.
41. Zickermann V, Dröse S, Tocilescu MA, Zwicker K, Kerscher S, and Brandt U. Challenges in elucidating structure and mechanism of proton pumping NADH: ubiquinone oxidoreductase (complex I). *J Bioenerg Biomembr* 40: 475–483, 2008.

Address correspondence to:
Dr. Nanduri R. Prabhakar
Department of Medicine
Center for Systems Biology of O_2 Sensing
University of Chicago
Emergency Medicine, MC5068
5841 South Maryland Ave.
Chicago, IL 60637

E-mail: nanduri@uchicago.edu

Date of first submission to ARS Central, March 25, 2010; date of final revised submission, July 8, 2010; date of acceptance, July 10, 2010.

Abbreviations Used

AEBSF = 4-(2-aminoethyl) benzenesulfonyl fluoride hydrochloride
BAPTA = 1,2-bis(o-aminophenoxy)ethane-*N*,*N*,*N*′,*N*′-tetraacetic acid
GSH = reduced form of glutathione
GSSG = oxidized from of glutathione
IH_{60} = cells exposed to 60 cycles of intermittent hypoxia
IP = intraperitoneal
MnTMPyP = manganese(III) tetrakis(1-methyl-4-pyridyl) porphyrin
NAC = *N*-acetyl-cysteine
Nox = NADPH oxidase
PC12 = pheochromocytoma 12
ROS = reactive oxygen species